

## Fabrication of a graded-wavelength guided-mode resonance filter photonic crystal

Dennis W. Dobbs, Irena Gershkovich, and Brian T. Cunningham<sup>a)</sup>

*Department of Electrical and Computer Engineering, University of Illinois at Urbana-Champaign, 208 North Wright Street, Urbana, Illinois 61801 and Micro and Nanotechnology Laboratory, University of Illinois at Urbana-Champaign, 208 North Wright Street, Urbana, Illinois 61801*

(Received 19 May 2006; accepted 9 August 2006; published online 19 September 2006)

The authors report on the fabrication and characterization of a guided-mode resonance filter whose spectral reflectance features vary in a linear fashion as a function of position on the filter. This device was fabricated using nanoreplica molding in conjunction with a linearly graded TiO<sub>2</sub> thin film deposition. The magnitude of gradation of the thin film was approximately 85 nm over a distance of 26 mm, which resulted in the spectral location of the primary reflection feature of the filter to be nearly linearly graded spanning a range of 798–909 nm across the 26 mm surface.

© 2006 American Institute of Physics. [DOI: 10.1063/1.2356695]

The development of compact inexpensive optical devices that are capable of spatial separation of wavelength components from an incoming beam is desirable for spectroscopy and sensing for a variety of applications. While diffraction gratings and prisms are widely used for such purposes, other methods may perform wavelength filtering with low cost, small size, and high resolution over a specified wavelength range. In this work, we report the design and operation of a guided-mode resonance filter (GMRF) photonic crystal that is designed to separate the reflection of specific wavelength bands across the width of the component. The device structure is selected to eliminate lateral propagation of light so that narrowband reflection characteristics are maintained even though a nonuniformity of reflected wavelength is intentionally introduced. The reported device is fabricated in glass materials using an inexpensive replica molding process.

The phenomenon of guided-mode resonance in planar dielectric waveguide gratings was first reported by Wang *et al.*<sup>1</sup> in 1990. In 1992, Magnusson and Wang<sup>2</sup> suggested that GMRFs represent a basic new optical element, with possible practical applications in polarization-sensitive filtering, low-power electro-optic switching, and high-precision sensing. A GMRF-based electro-optic modulator was demonstrated by Sharon *et al.*<sup>3</sup> in 1996, and the use of a GMRF as an optical biosensor was reported in 2002 by Cunningham *et al.*<sup>4</sup> Conceptual developments concerning the use of a GMRF as an all-optical switching device were presented by Boye *et al.*<sup>5</sup> in 1999 and by Mizutani *et al.*<sup>6</sup> in 2005. Recently, Dobbs and Cunningham<sup>7</sup> have reported on the fabrication of an optically tunable GMRF.

When the GMRF design described in this work is illuminated with broadband light at normal incidence with the light polarization perpendicular to the grating lines (TM polarization), a narrow band of wavelengths is strongly reflected. The spectral location of the reflection peak, which we will refer to as the peak wavelength value (PWV), is a sensitive function of all of the dimensions and refractive indices of the GMRF. In this work, we report on the fabrication and characterization of a static GMRF that exhibits a spa-

tially dependent PWV. The device, shown in Fig. 1, consists of a one-dimensional periodic surface structure fabricated on a low refractive index glass substrate that is overcoated with a thin film of high refractive index TiO<sub>2</sub>. As shown in the figure, the period of the structure is 550 nm, and the step height is approximately 170 nm. In this work, the thickness of the TiO<sub>2</sub> film is deliberately graded across the lateral direction of the substrate, such that the TiO<sub>2</sub> thickness is approximately 160 nm at lateral position  $x=0.0$  mm and is linearly varied to a thickness of approximately 245 nm at lateral position  $x=26.0$  mm. This results in a PWV of 798 nm at position  $x=0.0$  mm, and a PWV of 909 nm at position  $x=26.0$  mm.

As has been mentioned, the periodic surface structure was fabricated using a replica molding process. This process has been previously described in detail,<sup>8</sup> so only a brief summary will be presented here. First, a master of the grating pattern with a  $\sim 50/50$  duty cycle is fabricated on a silicon wafer using photolithography and plasma etching techniques. Then, a thin layer of uncured polydimethylsiloxane (PDMS) is poured onto the silane-treated silicon master, and the PDMS is cured for several hours in a 90 °C oven. After curing, the PDMS stamp is peeled off of the silicon master and set aside. Next, a 600 nm layer of sol-gel nanoporous glass (Nanoglass low- $k$  dielectric, Honeywell) is spun on to a clean glass microscope slide at 2000 rpm for 30 s. The PDMS stamp is then pressed into the uncured Nanoglass, and the sol gel is cured using a three-step hot plate baking process, with the PDMS stamp being removed after the first step. Finally, the low refractive index periodic surface structure is overcoated with a thin film of high refractive index TiO<sub>2</sub>.

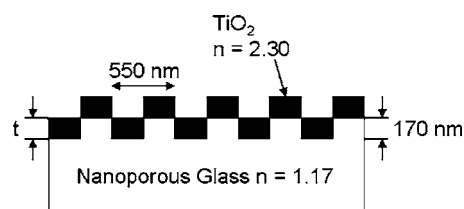


FIG. 1. Cross-section illustration of the fabricated GMRF.

<sup>a)</sup>Electronic mail: bcunning@uiuc.edu

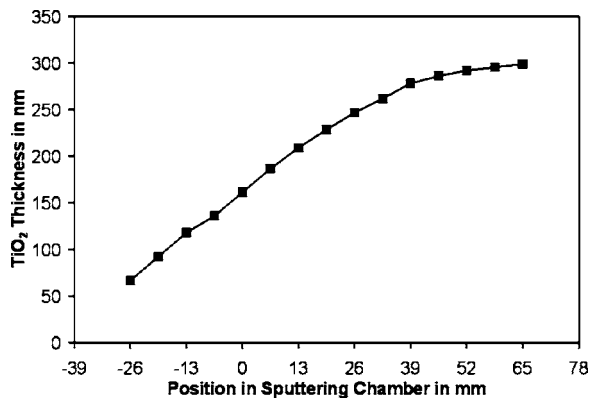


FIG. 2. Measured TiO<sub>2</sub> thickness at various positions in the sputtering chamber. The GMRF was positioned in between  $x=0$  mm and  $x=26$  mm, resulting in a nearly linear TiO<sub>2</sub> thickness gradient spanning 160 and 245 nm.

To deposit the graded-thickness TiO<sub>2</sub> film, we utilized the highly directional nature of rf sputtering (CV301, Cooke Vacuum Products). A 4 in. diameter TiO<sub>2</sub> sputtering source is on the bottom of the chamber facing upwards, and the microscope slide sample is mounted on the top of the chamber facing downwards, with the microscope slide sample positioned off to the side and out of the direct vertical sputtering path. It is in this region that deposited TiO<sub>2</sub> thickness is nearly linearly graded. For our sputter deposition, we utilized an argon pressure of 10 mTorr, an argon flow rate of 8 SCCM (SCCM denotes cubic centimeter per minute at STP), a rf power of 200 W, and a sputtering time of 90 min. In Fig. 2, the thickness of deposited TiO<sub>2</sub> is plotted versus position in the chamber. These data were obtained by placing a silicon wafer in the chamber during a deposition, and using variable angle spectroscopic ellipsometry (Woollam Co.) to determine the TiO<sub>2</sub> thickness at several locations on the silicon wafer. The patterned region of our GMRF sample was situated in between  $x=0.0$  mm and  $x=26.0$  mm. From Fig. 2, it is clear that the thickness of deposited TiO<sub>2</sub> at  $x=0.0$  mm is approximately 160 nm, and the thickness of deposited TiO<sub>2</sub> at  $x=26.0$  mm is approximately 245 nm. It is also evident that this gradient is quite linear in this region. For clarity, we also note that the region in between  $x=52.0$  mm and  $x=65.0$  mm is directly above the sputtering source, and thus the TiO<sub>2</sub> thickness does not have a significant gradient. Although replica molding procedures maintain sharp contours, the TiO<sub>2</sub> deposition results in slight rounding of the final surface structure and <20 nm of deposition on the vertical surfaces. Therefore, the fabricated structure differs slightly from the idealized cross section of Fig. 1. Scanning electron microscopy analysis reveals a lack of surface roughness, particularly at the size scale of the resonant wavelength.

The result of fabricating a GMRF with a graded thickness of TiO<sub>2</sub> is that the spectral location of the reflection peak is dependent on spatial position on the GMRF. This is illustrated in Fig. 3, which shows the measured reflected intensity at six different positions on the GMRF, from  $x=0.0$  mm to  $x=26.0$  mm. At  $x=0.0$  mm, the PWV is approximately 798 nm, and at  $x=26.0$  mm, the PWV is approximately 909 nm, giving a 111 nm PWV gradient. The relationship between PWV and spatial location on the GMRF is quite linear, owing to the nearly linear TiO<sub>2</sub> thickness gradient, and the fact that the relationship between TiO<sub>2</sub>

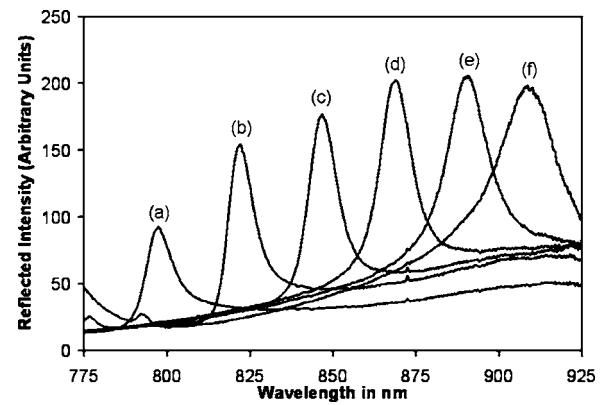


FIG. 3. Measured normal-incidence reflectance spectra with TM polarization at six locations on the GMRF. The positions measured were (a) 0.0 mm, (b) 5.2 mm, (c) 10.4 mm, (d) 15.6 mm, (e) 20.8 mm, and (f) 26.0 mm. Corresponding PWVs at these locations are (a) 798 nm, (b) 822 nm, (c) 847 nm, (d) 869 nm, (e) 891 nm, and (f) 909 nm. At a wavelength of 855 nm, the measured reflection efficiency with respect to an aluminum mirror is 75%.

thickness and PWV is linear, as is discussed below. Another interesting feature of the GMRF we have fabricated is that it exhibits two TM resonances. This is illustrated in Fig. 4, which shows the measured normal-incidence reflection spectrum obtained at a position of  $x=15.6$  mm on the GMRF. As can be seen in the figure, the two TM reflection resonances are located at 720 and 869 nm. Insight into the physical explanation for the presence of two TM resonances can be obtained by inspection of Fig. 1. It is clear that the fabricated GMRF can be thought of as containing two distinct planar dielectric gratings in the lateral direction: the Nanoglass-TiO<sub>2</sub> grating and the air-TiO<sub>2</sub> grating. Thus, each effective grating has its own characteristic resonance. The data presented in Figs. 3 and 4 were obtained using a two-fiber reflectance probe and collimating lens set at normal incidence to the GMRF and with the incident polarization set to TM. Light from a broadband tungsten-halogen source (LS-1, Ocean Optics) is sent through the incident fiber, and reflected light is collected in the probe fiber and is sent to a near infrared spectrometer (USB 2000, Ocean Optics).

For purposes of comparison, we have also performed numerical calculations of the spectral properties of the graded-wavelength GMRF. For these calculations, we utilized the rigorous coupled wave analysis (RCWA) method. The RCWA method, first reported by Moharam and Gaylord<sup>9</sup>

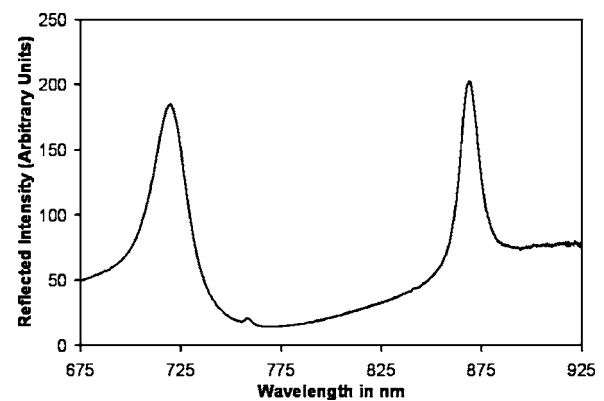


FIG. 4. Measured normal-incidence TM-polarization reflection spectrum at a location of  $x=15.6$  mm on the GMRF. The two resonances are located at 720 and 869 nm.

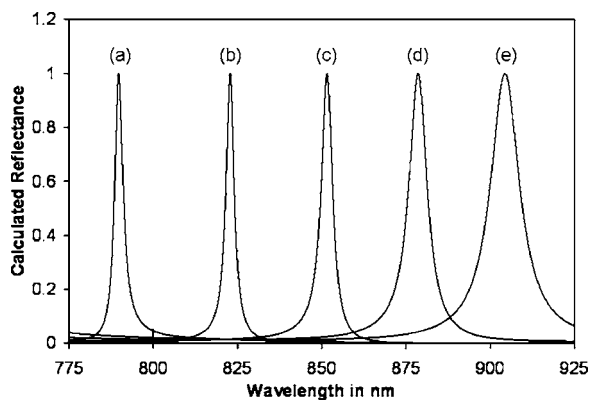


FIG. 5. Calculated normal-incidence TM-polarization reflectance spectra for the structure illustrated in Fig. 1 for  $\text{TiO}_2$  thicknesses of (a) 160 nm, (b) 180 nm, (c) 200 nm, (d) 220 nm, and (e) 240 nm, resulting in PWVs of (a) 790 nm, (b) 823 nm, (c) 852 nm, (d) 879 nm, and (e) 904 nm.

in 1981, is a technique for obtaining a near-exact solution to Maxwell's equations for periodic diffracting structures. In this work, we utilized a commercially available implementation of the RCWA technique (DIFFRACTMOD, RSoft Corporation). Figure 5 shows calculated normal-incidence reflectance spectra at TM polarization for the device model illustrated in Fig. 1 for five different values of the  $\text{TiO}_2$  thickness, ranging from 160 to 240 nm in increments of 20 nm. This figure illustrates the considerable sensitivity of PWV to changes in the  $\text{TiO}_2$  thickness. In addition, it is apparent that the relationship between PWV and  $\text{TiO}_2$  thickness is quite linear. Another interesting feature of this calculation is that the spectral width of the peak tends to broaden as the  $\text{TiO}_2$  thickness is increased. This behavior is also somewhat evident in the measured spectra of Fig. 3. Furthermore, comparison of the spectral location of the reflection peaks between the measured spectra of Fig. 3 and the calculated spectra of Fig. 5 reveals satisfactory agreement. Comparison of these two figures also reveals that the measured spectral widths of the reflection peaks are significantly wider than the calculated spectral widths. This is primarily due to the fact that the beam spot diameter used in measurement was approximately 3 mm, resulting in a significant range of

PWVs in any given measured spot. Also, from inspection of Fig. 3 it is apparent that the diffraction efficiency is not constant across the surface of the GMRF, especially for the case of the  $x=0$  mm measurement position. This may be due to local regions of poor replication during device fabrication.

It is interesting to note that the RCWA technique assumes that periodic boundary conditions apply. Since our graded-wavelength GMRF has a graded  $\text{TiO}_2$  thickness, it is not periodic in an exact sense. However, our experimental results indicate that with a gradient as shallow as ours, the assumption of perfect periodicity is still an excellent local approximation. In fact, the gradient is so shallow that there are 556 grating periods for every 1 nm change in  $\text{TiO}_2$  thickness.

In summary, we have simulated, fabricated, and characterized a graded-wavelength GMRF. Fabrication of the device was performed using a nanoreplica molding process in conjunction with a graded thin film deposition. Through a 85 nm linear gradation in the thickness of the  $\text{TiO}_2$  film across a 26 mm distance, the spectral location of the reflection peak of the fabricated GMRF was found to vary nearly linearly across a spectral range of 111 nm.

This work was supported by the National Science Foundation under Grant No. 0427657. Any opinions, findings, and conclusions or recommendations expressed in this material are those of the author(s) and do not necessarily reflect the views of the National Science Foundation.

<sup>1</sup>S. S. Wang, R. Magnusson, J. S. Bagby, and M. G. Moharam, *J. Opt. Soc. Am. A* **7**, 1470 (1990).

<sup>2</sup>R. Magnusson and S. S. Wang, *Appl. Phys. Lett.* **61**, 1022 (1992).

<sup>3</sup>A. Sharon, D. Rosenblatt, A. A. Friesem, H. G. Weber, H. Engel, and R. Steingrueber, *Opt. Lett.* **21**, 1564 (1996).

<sup>4</sup>B. Cunningham, B. Lin, J. Qiu, P. Li, J. Pepper, and B. Hugh, *Sens. Actuators B* **85**, 219 (2002).

<sup>5</sup>R. R. Boye, R. W. Ziolkowski, and R. K. Kostuk, *Appl. Opt.* **38**, 5181 (1999).

<sup>6</sup>A. Mizutani, H. Kikuta, and K. Iwata, *J. Opt. Soc. Am. A* **22**, 355 (2005).

<sup>7</sup>D. W. Dobbs and B. T. Cunningham, *Appl. Opt.* **45**, (2006).

<sup>8</sup>I. D. Block, L. L. Chan, and B. T. Cunningham, *Sens. Actuators B* (to be published).

<sup>9</sup>M. G. Moharam and T. K. Gaylord, *J. Opt. Soc. Am.* **71**, 811 (1981).